On the Simulation of Cooling Curves Using Simple Functional Formats

Zoltán Fried[†], Imre Felde[‡], József K. Tar[⋆]

[†]Doctoral School of Applied Informatics and Applied Mathematics,
[‡]Smartlab Knowledge Center,
[⋆]Antal Bejczy Center for Intelligent Robotics (ABC iRob),
University Research, Innovation and Service Center,
Óbuda University, H-1034 Budapest, Bécsi út 96/B, Hungary
E-mail: zoltan.fried@deirf.hu, felde@uni-obuda.hu, tar.jozsef@nik.uni-obuda.hu

Abstract: Quenching of metal products is a complex physical process that is difficult to precisely describe by physical models. The "Heat Transfer Coefficient (HTC)" at the surface of the workpiece is a practical parameter that depends on the nature of the flow, the density, viscosity, and the thermal properties of the cooling liquid, the surface quality, shape, and thermal data of the component under quenching. Normally only numerical techniques are available for its estimation that need huge computational power. However, in the practice, on the basis of approximate quantitative data and some qualitative knowledge, often good and simple approximations can be elaborated for the description of quite complicated problems. In this paper a simple approximation is suggested for modeling the time-dependence of the HTC of an Inconel 600 alloy probe of cylindrical shape used in the standard ISO 9950. Simulation results using moderate computational power are presented to substantiate the suggestion.

Keywords: Quenching; Heat Transfer Coefficient; Finite Elements Methods; Newton-Raphson Algorithm; Julia

1 Introduction

Quenching of metal products is a complex physical process that is difficult to precisely describe by physical models. The HTC at the surface of the workpiece is a practically introduced parameter that depends on the nature of the bulk flow (laminar or turbulent), the temperature, density, viscosity, and the thermal properties of the cooling liquid, the surface quality, shape, and the thermal data of the component under quenching. Normally only numerical techniques are available for its estimation that need huge computational power. The "direct" problem, i.e. determining the temperature distribution versus time of the probe for a given initial distribution and the boundary conditions if the function $HTC(\mathbf{r},t)$ is given in advance (t denotes

the time, and $\mathbf{r}$ means the location over the surface of the sample), has an unique solution. However, the "inverse problem", i.e. finding the function $HTC(\mathbf{r},t)$ over the sample's surface in the possession of the temperature distribution $T(\mathbf{r},t)$ in certain points of the quenched sample is a more complicated task that generally is an "ill-posed" problem as it was observed by Beck et al. in 1985 [1]. Generally neither the uniqueness, nor the stability of the solution can be guaranteed.

Mathematically the problem can be defined as an optimization task in which on the basis of some assumed $HTC(\mathbf{r},t)$ distribution the cooling curves in certain points within the probe are calculated, and some cost function that measures its distance from the available measured data is minimized by modifying the assumed distribution (e.g. [1, 2, 3, 4, 5, 6, 7]).

The complexity of the task can be considerably reduced if samples of particular shapes and special locations for temperature measurements are chosen. On this reason the standard ISO 9950 [8] uses special cylindrical samples with measurement points in the centerline of the cylinder. Further simplification of the calculations is possible if during the quenching process no latent heat appears that in general can be caused by either phase transitions or chemical reactions within the probe. These advantages are guaranteed by the special alloy (Inconel 600) that is recommended by the standard, and for which well known thermal data are available in the temperature range of the investigations [9]. Since the process still has ample difficulties due to the behavior of the cooling liquid, even if geometric simplifications are applied, high computational requirements remain that make it expedient to use evolutionary techniques as well as the utilization of the various hardware components of the computers as the computational capacity of the graphical cards (e.g. [10, 11, 12, 13, 14]).

However, in the practice, on the basis approximate quantitative data and some qualitative knowledge, often good and simple approximations can be elaborated for the description of quite complicated problems. A mathematically rigorous approach is the application of fuzzy sets [15] that can be used for modeling and control applications (e.g. [16, 17, 18, 19]). The essence of this approach is that by the use of the available qualitative and quantitative information, membership functions and operators of certain particular form (e.g. [20]), special models can be constructed that well capture and mirror the essential properties of the phenomenon under consideration. Though the very particular properties of these special models are not well or uniquely determined, in the practice they can be successfully applied.

In this paper a simple approximation is suggested for modeling the time-dependence of HTC of an Inconel 600 alloy probe of cylindrical shape used in the standard ISO 9950. The basic idea is that instead trying to use some particular temporal distribution of $HTC(\mathbf{r},t)$ over the surface of the sample, on the basis of qualitative considerations it is assumed that the HTC at the surface of the probe *physically must depend on* the surface temperature of the probe as $HTC(T(\mathbf{r},t))$, and the function $HTC(T)$ depends only on a few "shape parameters". The shape of this function can be formally defined and tuned by modifying only a few shape parameters. This approach reduces the complexity of the problem to a great extent and allows the application of simple optimum seeking algorithms that can be implemented on even low ca-

pacity computers. Accordingly, simulation results using moderate computational power are presented to substantiate the suggestion. The computations were made on a **Dell inspiron 15R laptop** operated by the central processor Intel® Core™ i5-3337U CPU @ 1.80GHz × 4 under an Ubuntu ver. 13.04 operating system without using any graphical computational power. The sequential program was written in Julia Version 1.0.3 (2018-12-18). This program language is developed at the MIT, it is very similar to the MATLAB, but it runs almost as fast as a C code (benchmarking data are available at [21], Fig. 1).

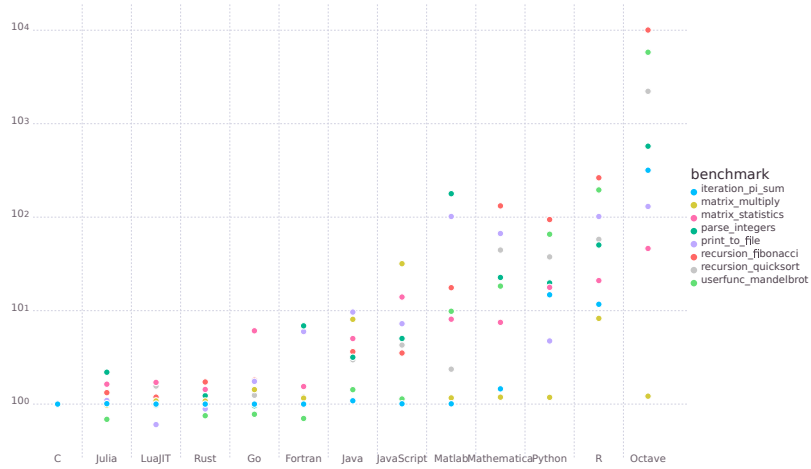

Figure 1
Some benchmarking data for language Julia (source: [21])

2 The Dynamic Model and Its Finite Elements Approximation for Long Cylindrical Samples

The quenched sample considered in the simulations was made of the alloy "Inconel 600" that, in the range of the investigations, does not produce measurable latent heat that generally can be produced by either phase transitions or chemical reactions. On this reason this alloy is used in the standard ISO 9950 [8]. This standard also determines the geometric properties of the sample: it must have a cylindrical shape in the symmetry axis in which the temperature sensors can be located. Normally, due to the cylindrical symmetry of this sample, mathematically we have to consider a two dimensional problem with the independent variables that describe the location of the considered point in the direction of the symmetry axis, and in the radial direction. However, if the sample is "long", and it is evenly immersed into the quenching liquid, at the axial level of its central point no heat drift can be assumed in the axial direction, and the problem can be reduced into a single variable one. In the sequel this model of reduced complexity is investigated under the name *"Long Cylindrical Sample"*. It is important to emphasize that this approximation cannot be applied for the description of the cooling process at the points that are not located at the cenral axial level: in this case the effects of the "upper" and "lower" boundaries of the

cylinder of finite size have nonsymmetric effects, and the problem must be treated as a 2 dimensional one. Furthermore, if the possible deformation of the sample in the three dimensional space has to be considered, too, in general a three dimensional problem has to be considered.

2.1 The "Long Cylindrical Sample" Approximation

In this approximation the concept of "long sample" means that no energy transfer in the axial direction is assumed. Furthermore, by assuming cylindrical symmetry, a single dimensional heat transfer equation can be considered as in [11, 22], and the heat conduction equation is reduced to (1)

$$\frac{\partial}{\partial r}\left(k(T(r,t))\frac{\partial T(r,t)}{\partial r}\right)+\frac{k(T(r,t))}{r}\frac{\partial T(r,t)}{\partial r}=\rho C_p(T(r,t))\frac{\partial T(r,t)}{\partial t}\quad , \tag{1}$$

in which $t\,[s]$ denotes the time, $r\,[m]$ denotes the radius from the centerline as the "independent variables" of the problem, $T\,[C]$ is the temperature. The numerical properties of the alloy Inconel 600 were taken from [9] as $\rho = 8420\,\left[kg\,m^{-3}\right] \equiv const.$ For the *"heat conductivity coefficient"* $k(T)\,\left[J\,s^{-1}\,m^{-1}\,K^{-1}\right]$ and the *"specific heat at constant pressure"*, $C_p(T)\,\left[J\,kg^{-1}\,K^{-1}\right]$ third order polynomials were fitted in the range $T \in [27, 796.45]\,[C]$ for the tabulated data as it is given in Fig. 2.

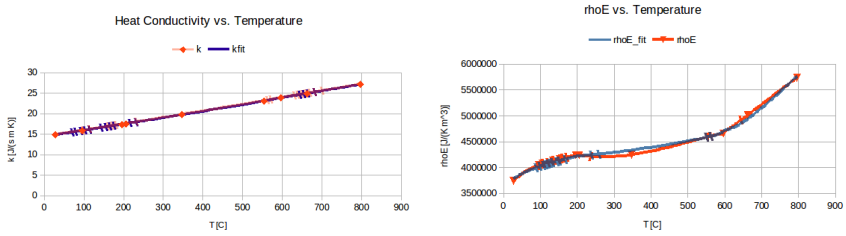

Figure 2
The dependence of the "heat conductivity coefficient" (LHS) and $\rho_E \equiv \rho C_p$ (RHS) on the temperature in (1): fitted 3rd order polynomials for the tabulated data published for Inconel 600 in [9]

For (1) the appropriate *boundary conditions* were set for the sample of radius $R = 6.25\,[mm]$ as

$$-k(T(R,t))\left.\frac{\partial T(r,t)}{\partial r}\right|_{r=R} = h(t)(T(R,t)-T_q)\quad , \tag{2}$$

in which $T_q\,[C]$ is the temperature of the bulk quenching liquid in turbulent flow, and $h(t)\,\left[J\,s^{-1}\,m^{-1}\,K^{-1}\right]$ is the *heat transfer coefficient* of the boundary layer of the liquid at the surface of the probe that is assumed to vary in time as the sample cools down. Besides the boundary condition equation (1) must be completed with the *initial conditions*. The *initial conditions* must be compatible with the *boundary conditions*. This compatibility must be guaranteed at the level of the *finite elements approximation* of the equations that are detailed in the Subsection 2.2.

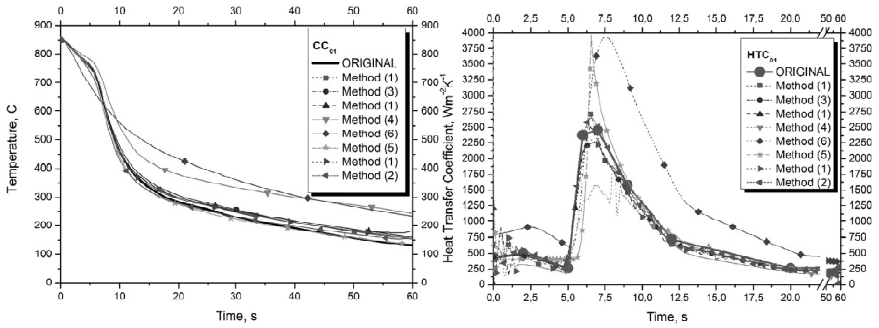

Figure 3
Cooling curves and HTC values calculated with various approximation methods for the 12.5 $[mm]$ diameter cylindrical probe made of Inconel 600 (Figs. 7 and 4 in [22])

To make the calculations realistic already known data were taken from the literature to extract qualitative and approximate quantitative knowledge for the probe considered (Fig. 3). The initial temperature $T_{ini} = 850\,[C]$ is a little bit higher than the maximal value in [9] (796.45 $[C]$), however, the small difference allowed the use of the fitted polynomials in Fig. 2 for *data extrapolation* outside the range of fitting.

2.2 The Finite Elements Approximation of The Problem

Evidently, due to the singularity of the polar system of coordinates at $r = 0$ the center of the sample cannot be numerically considered. To evade this problem instead of the *exact range* $[0,R]$ the range $[\Delta r,R]$ was so considered that the $[0,R]$ interval was divided into $N \in \mathbb{N}$ equally long intervals as $\Delta r = \frac{R}{N}$, and in the role of the center line $r = \Delta r$ was placed. For the grid points $\{r_i | i = 2,\ldots,N-1\}$ the *central estimation of the gradient* was used as in (3a). Consequently, the numerical calculation of $\nabla(k \cdot \nabla T)$ in (1) was possible for the points $\{r_i | i = 3,\ldots,N-2\}$ in (3b), and for the "center line" the approximation in (3c) was applied. This means that $\frac{\partial T}{\partial t}$, therefore the direct refreshment of the temperature values during an Euler integration, was possible only for the points $\{r_i | i = 3,\ldots,N-2\}$, too.

$$\frac{\partial T(r_i,t)}{\partial r_i} \approx \frac{T(r_{i+1},t) - T(r_{i-1},t)}{r_{i+1} - r_{i-1}} \quad i \in \{2,\ldots,N-1\} \tag{3a}$$

$$\frac{\partial}{\partial r}\left(k\frac{\partial T}{\partial r}\right) \approx \frac{k(r_{i+1},t)\nabla T(r_{i+1},t) - k(r_{i+1},t)\nabla T(r_{i-1},t)}{r_{i+1} - r_{i-1}} \quad i \in \{3,\ldots,N-2\} \tag{3b}$$

$$T(r_1,t) \equiv T(r_2,t) \equiv T(r_3,t) \tag{3c}$$

To solve the boundary conditions in (2) a *refreshed value* T in grid point r_{N-1} was estimated by using the 1st spatial derivative of the already refreshed points as in (4)

$$T(r_{N-1},t) \approx T(r_{N-2},t) + \frac{(r_{N-1} - r_{N-2})(T(r_{N-2},t) - T(r_{N-3},t))}{(r_{N-2} - r_{N-3})} \quad , \tag{4}$$

and $T(r_N,t)$ was estimated by the use of the heat transfer coefficient as in (5)

$$T(r_N,t) \approx \frac{h(T(r_{N-1},t))T_q + k(T(r_{N-1},t))/\Delta r}{h(T(r_{N-1},t)) + k(T(r_{N-1},t))/\Delta r} \quad . \tag{5}$$

2.3 Setting The Parameters of The Numerical Calculations

For the simulations the *functional format* for describing the dependence of the HTC on the surface temperature the function given in (6) was applied

$$h(T) = h_{max} \begin{cases} \exp\left(-([T - T_{max}]/w_{left})^p\right) & \text{if } T <= T_{max} \\ \exp\left(-([T - T_{max}]/w_{right})^p\right) & \text{if } T > T_{max} \end{cases}, \tag{6}$$

in which h_{max} denotes an assumed possible maximal HTC value, T_{max} denotes the surface temperature that belongs to the "location" of this maximum, and the width parameters w_{left} and w_{right} belong to asymmetric solutions. The parameter p determines the nature of the "tail" of the function, it was kept fixed when the gradient was computed. This format was selected on the basis of plausible physical considerations that are relevant in the refrigeration industry that has to cope with similar problems though in a much lower temperature range than that of the steel industry. However, this lower range allows the application of tubes made of glass allowing simple optical observations that are not available in the steel industry (e.g. [23, 24, 25]). The HTC is a *practically well measurable parameter* behind which complicated physical processes are hidden as follows.

a) The cooling liquid normally has turbulent flow that allows very efficient heat transfer between the stirred fluid layers with the exception at the boundary layer of the quenched sample. The liquid sticks on the surface of the sample, due to that a thin film (the "boundary layer") is formed around the sample within which the flow is laminar. Within this layer the heat transfer happens mainly via heat conduction that is not an efficient form of the heat transfer. This process is concerned by the quality of the surface of the probe, too.

b) The viscosity of the liquid decreases with increasing temperature, due to which at higher temperatures thinner films with better heat transfer ability are expected.

c) When the temperature achieves the boiling point of the liquid at the pressure of the operation, at the surface of the probe gas bubbles appear that act as "heat insulators", so at higher temperatures some decrease in the HTC value is expected.

Precise modeling of the above phenomena is very difficult, however, they substantiate the use of the simple asymmetric form defined in (6). It is also reasonable to expect that by fitting the 4 independent parameters in (6) good approximate modeling possibility can be created. It worths noting that in the practice complicated function expressions can be quite well approximated by simple ones. For example the normal, the epsilon, and the omega distributions were well approximated by simple function formats by Dombi et al. in [26, 27, 28], as well as the kappa regression function in [29].

Really, it was easy to find qualitatively acceptable approximation of the curves in Fig. 3 by using (6) with the "target parameters" in Table 1. By printing the results for the same graphs when in Subsection 2.2 the pairs $\{N = 50, \delta t = 10^{-3}\,[s]\}$ and $\{N = 20, \delta t = 10^{-2}\,[s]\}$ were selected (δt is the time-resolution of a simple Euler

integration according to the time variable), Fig. 4 was obtained. The differences between the results are not too drastic, therefore in the further investigations the "faster settings", i.e. $\{N = 20, \delta t = 10^{-2}\,[s]\}$ were used. (It can be noted that according to Fig. 3 obtained from the litearture, the various methods provided considerably different results.)

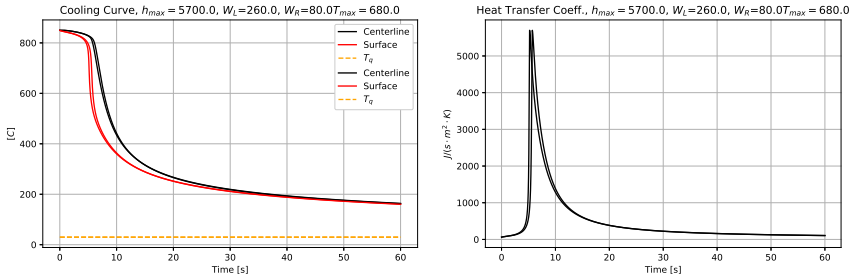

Figure 4
The "Cooling Curve" and the "HTC versus Time" functions belonging to Eq. (6), the "Target" parameters given in Table 1, and the numerical parameter pairs $\{N = 50, \delta t = 10^{-3}\,[s]\}$ and $\{N = 20, \delta t = 10^{-2}\,[s]\}$ in Subsection 2.2

Table 1
The applied "target" and "initial" model parameters in (6)

Parameter	**Target**	**Initial**
h_{max} $\left[J\,s^{-1}\,m^{-2}\,K^{-1}\right]$ HTC	5700.0	5500.0
T_{max} $[C]$ location of maximal HTC	680.0	650.0
w_{left} $[C]$ left width	260.0	300.0
w_{right} $[C]$ right width	80.0	60.0
p [nondimensional] "tail property" parameter (fixed)	2.0	2.0

3 Simulation Results

By the use of the above approximations, for the given $T_q = 30.0\,[C]$ cooling liquid temperature, $T_{ini} = 850.0\,[C]$ initial probe temperature, the cooling curve over the time-grid $\delta t[1,6000]$ a multiple variable multiple output function can be obtained with *a* 4 *dimensional input space* consisting of the input variables defined in Table 1. By defining the error as the Frobenius norm of the difference of "Target Temperature vs. Time" and the "Simulated Temperature vs. Time" functions as $E(x) : \mathbb{R}^4 \mapsto \mathbb{R}$ can be created the minimum of which has to be found for determining the $HTC(t)$ function. While the numerical implementation of the standard "Reduced Gradient Method" that originally was invented by Lagrange in 1811 [30] for use in the formulation of Classical Mechanics may result in slow algorithm if no information we have on the expected minimum of $E(x)$ (in this case no reduction of the gradient was

necessary in the lack of constraints), the classical Newton-Raphson algorithm (e.g. [31]) may result in fast solution if the assumption $\min E(c) = 0$ is made. The basic idea is as follows: select an initial point $x(1)$, calculate $\nabla E(x(1))$, and make a big step $\Delta x = \alpha \nabla E(x(1))$ so that $-E(x(1)) = \Delta x^T \nabla E(x(1))$. Then repeat the procedure at $x(2) = x(1) + \Delta x$, etc. Roughly speaking, it is expected that already the 1st step almost makes $E(x)$ well approximate zero. For this the selection

$$\alpha = \frac{-E(x(1))}{\|\nabla E(x(1))\|^2} \tag{7}$$

is needed. However, it is well known that if ∇E is not precisely computed, this algorithm easily can diverge without finding the minimum. In our case the gradient is only very imprecisely estimated, so the original Newton-Raphson algorithm was modified as its is described in Subsection 3.1.

3.1 The Modified Newton-Raphson Algorithm for the Problem Having Exact Solution

The modification of (7) is given in (8)

$$\alpha = \gamma \frac{-E(x(1))}{\|\nabla E(x(1))\|^2 + \varepsilon} \ , \tag{8}$$

in which $\varepsilon = 10^{-14}$ was introduced to evade division by zero, and the "refining factor" $\gamma = 5 \times 10^{-3}$ was experimentally set. For the estimation of the components of $\nabla E(x)$ the "actual values" in Table 1 were modified as $h_{max} \to h_{max} + \Delta h_{max}$, $T_{max} \to T_{max} + \Delta T_{max}$, $w_{left} \to w_{left} + \Delta w_{left}$, and $w_{right} \to w_{right} + \Delta w_{right}$ with $\Delta h_{max} = 10^{-3} \left[J\, s^{-1}\, m^{-2}\, K^{-1} \right]$, $\Delta T_{max} = 10^{-3}\ [K]$, $\Delta w_{left} = 10^{-3}\ [K]$, and $\Delta w_{right} = 10^{-3}\ [K]$. The differences between the neighboring values were computed for the estimation of the components of the gradient of $E(x)$.

The parameter of γ from the initial value 1 (that corresponds to the original Newton-Raphson algorithm) was decreased till the algorithm ceased to "jump" between large final errors. This solution forms a "transition" between the fast Newton-Raphson algorithm and the slower "Gradient Descent" method, and it allows a practical compromise between the precision and the running time.

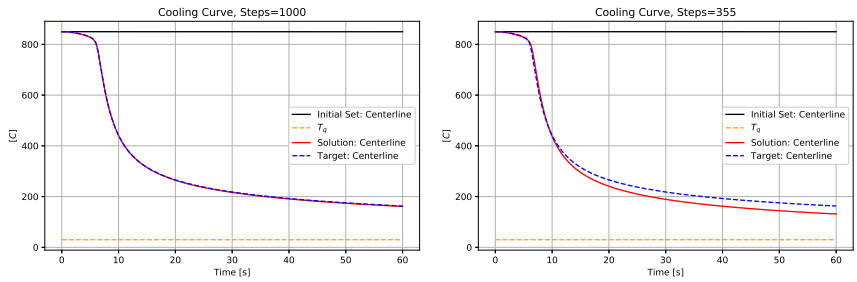

Figure 5
The operation of the modified Newton-Raphson algorithm for the problem having exact solution, i.e. the model defined in Eq. (6) with the parameters given in Table 1: the "Cooling Curves" for 1000 steps (LHS), and for limited precision achieved by stopping the algorithm at a lower error-limit 2000 (RHS)

To check the suggested method's abilities for target distributions that slightly differ from the "target form" (6), the target distribution generated by (9) was applied in which a "deformation parameter" $D = 7.5 \times 10^{-2}$ was introduced.

$$h(T) = h_{max} \begin{cases} \frac{D}{D+([T-T_{max}]/w_{left})^p} & \text{if } T <= T_{max} \\ \frac{D}{D+([T-T_{max}]/w_{right})^p} & \text{if } T > T_{max} \end{cases}, \tag{9}$$

By the use of the same common parameters in (6) and (9), the effect of the introduction of the above parameter D is revealed by Fig. 8 in which the appropriate cooling curves and the HTC vs. time functions are plotted in the same diagrams.

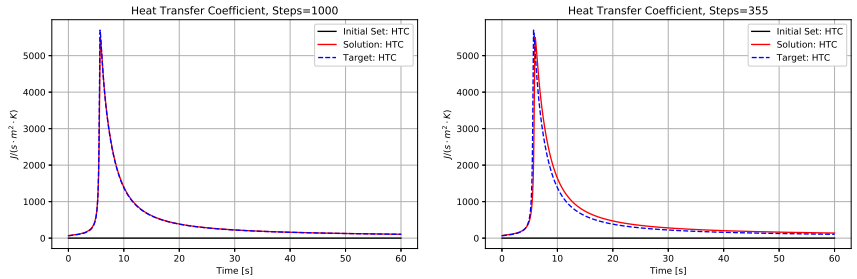

Figure 6
The operation of the modified Newton-Raphson algorithm for the problem having exact solution, i.e. the model defined in Eq. (6) with the parameters given in Table 1: the "HTC" value as the function of the time for 1000 steps (LHS), and for limited precisison achieved by stopping the algorithm at a lower error-limit 2000 (RHS)

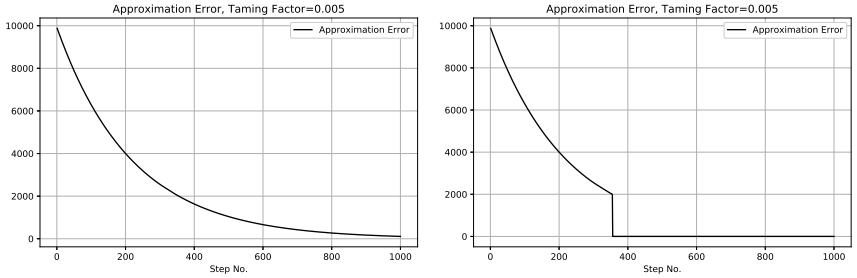

Figure 7
The operation of the modified Newton-Raphson algorithm for the problem having exact solution, i.e. the model defined in Eq. (6) with the parameters given in Table 1: the "approximation error" value as the function of the time for 1000 steps (LHS), and for limited precision achieved by stopping the algorithm at a lower error-limit 2000 (RHS)

3.2 The Modified Newton-Raphson Algorithm for the Problem Not Having Exact Solution

In these cases the "targets" and the "approximations" are generated by different format functions. Figure 9 reveals that though it was impossible to exactly reach the

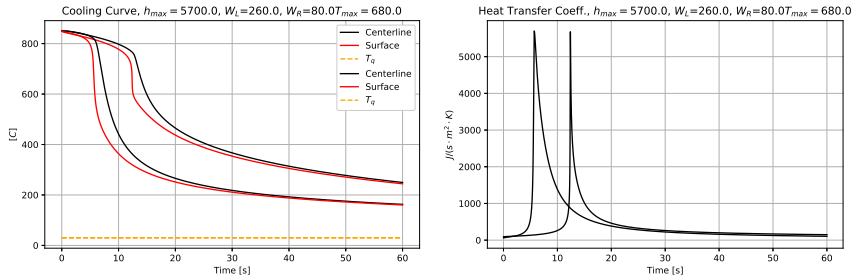

Figure 8
The effect of the "deformation parameter" $D = 7.5 \times 10^{-2}$ in the target distribution generated by Eq. (9) (LHS) and the appropriate functions $HTC(t)$ (RHS)

"target" distribution with the deformed functional shape, the algorithm well approximated the target, and the obtained $HTC(t)$ functions were comparable.

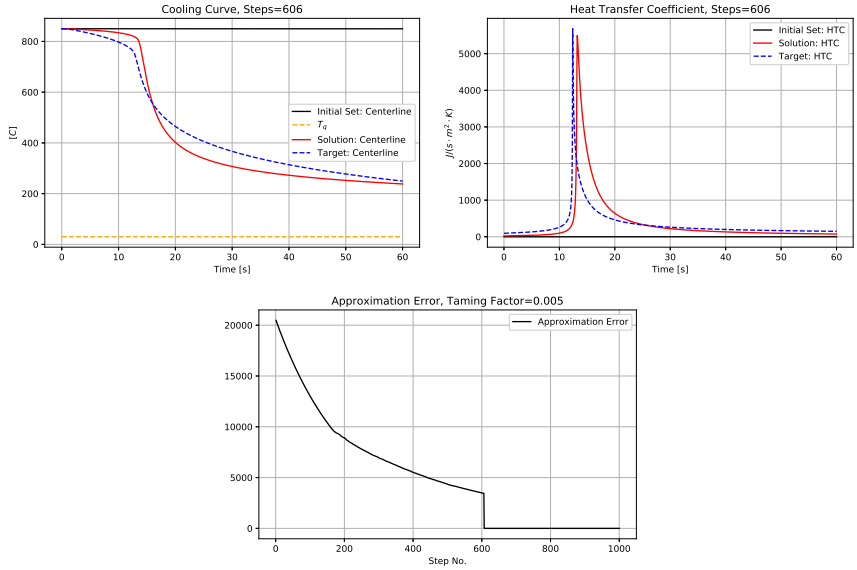

Figure 9
The operation of the modified Newton-Raphson algorithm for the problem that does not have exact solution: the lower error-limit was set to 1.0, the maximum step number was set to 1000. The algorithm stopped when further reduction of the error became impossible.

Regarding the computational efficiency of the suggested solution, the running time of the program must be measured. In the case of language Julia, the time need of the 1st execution of the program is not relevant because it contains the time necessary for the compilation of the program. However, the further runs' time need is free of the needs of the "preparatory" activities, and can be considered as a relevant measure of the speed of program execution. For obtaining the results in Fig. 9 approximately $9\,[min]\,22\,[s]$ computational time was necessary for the hardware and

software specified in Section 1.

For further improvement of the numerical approximations it seems to be a plausible way to apply asymmetric format functions. This modification of the format functions only slightly incerases the dimension of the space of the independent parameters. In the next subsection a simple example is considered.

3.3 Application of Asymmetric Format Functions

For this purpose it seems to be a plausible possibility to modify (6) by introducing different power parameters for the "left side" p_{left} and the "right side" p_{right} instead of the common power parameter p as in (10) and (9) as

$$h(T) = h_{max} \begin{cases} \exp\left(-([T - T_{max}]/w_{left})^{p_{left}}\right) & \text{if } T <= T_{max} \\ \exp\left(-([T - T_{max}]/w_{right})^{p_{right}}\right) & \text{if } T > T_{max} \end{cases}, \tag{10}$$

and

$$h(T) = h_{max} \begin{cases} \frac{D}{D+([T-T_{max}]/w_{left})^{p_{left}}} & \text{if } T <= T_{max} \\ \frac{D}{D+([T-T_{max}]/w_{right})^{p_{right}}} & \text{if } T > T_{max} \end{cases}, \tag{11}$$

Further tuning of these parameters increases the dimension of the search space only by 2 that expectedly does not mean significant effect on the complexity of the gradient-based simple approach. Typical function formats are revealed by Fig. 10 for a realizable, and Fig. 11 for an exactly not realizable case. The relaxation of the tracking error is described in Fig. 12.

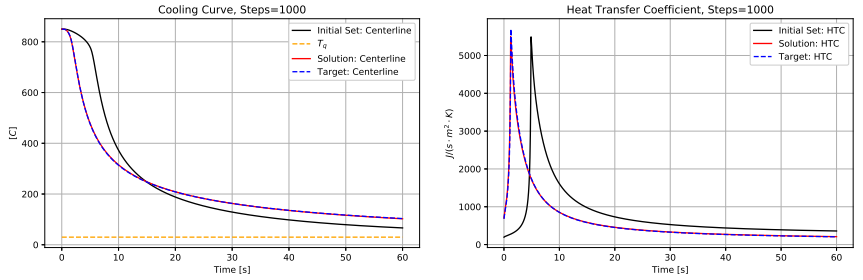

Figure 10
The operation of the modified Newton-Raphson algorithm for the problem having exact solution for asymmetric constant "tail property parameters" $p_{left} = 1.5$ and $p_{right} = 1.0$ in (10): the lower error-limit was set to 1.0, the maximum step number was set to 1000. The algorithm stopped when further reduction of the error became impossible.

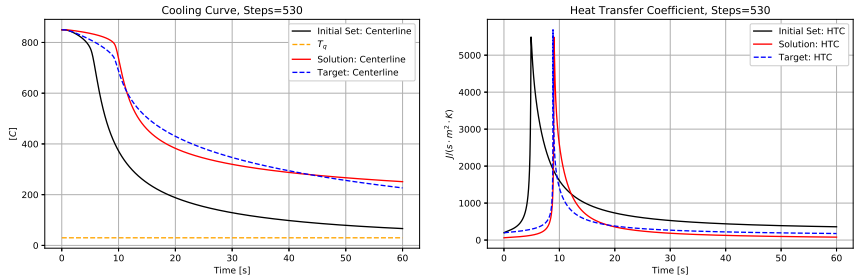

Figure 11
The operation of the modified Newton-Raphson algorithm for the problem that does not have exact solution for asymmetric constant "tail property parameters" $p_{left} = 1.5$ and $p_{right} = 1.0$ in (10) and (11): the lower error-limit was set to 1.0, the maximum step number was set to 1000. The algorithm stopped when further reduction of the error became impossible.

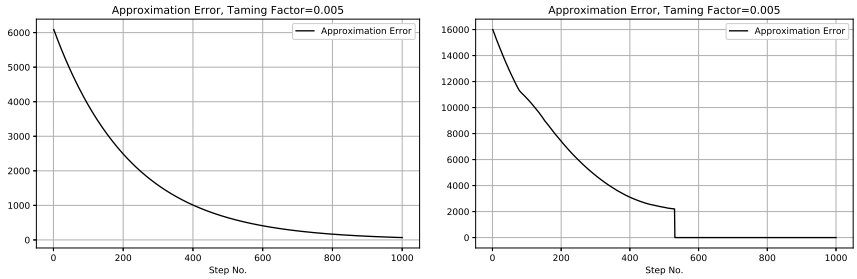

Figure 12
The error reduction during the application of the modified Newton-Raphson algorithm for asymmetric constant "tail property parameters" $p_{left} = 1.5$ and $p_{right} = 1.0$ in (10): the lower error-limit was set to 1.0, the maximum step number was set to 1000. (The algorithm stopped when further reduction of the error became impossible.) LHS: for the problem having exact solution (belonging to Fig. 10), RHS: for the problem not having exact solution (belonging to Fig. 11)

4 Conclusions

In this paper a simple computational method was suggested for the approximate determination of the HTC vs. time function from the cooling curve in the centerline of the cylindrical Inconel 600 probe recommended in the standard ISO 9950. In the applied approach "long cylinder" was considered that made it possible to use a single dimensional heat conduction equation by utilizing the cylindrical symmetry of the problem.

The main point of the approximation and problem simplification was the assumption that instead of an explicit function of the time the HTC distribution depends on the surface temperature distribution for which a simple single variable $HTC(T)$ function was introduced that contained only 4 "format parameters". The problem mathematically was formulated as a simple optimization task in which the 4 dimensional input space a scalar error function was minimized by an algorithm that corre-

sponds to a "transition" between the "Gradient Descent" and the "Newton-Raphson Algorithm". For checking the computational needs and speed of the method a fast language, the Julia was chosen for implementation that is almost as fast as a standard C code.

It was found that the problem was manageable with the given software and hardware combination. The method contains a single parameter that "tames" the originally rough steps of the Newton-Raphson algorithm and allows various compromises between the precision and computational time.

Further possibility is that instead of the scalar error $E(x)$ its gradient $\nabla E(x)$ can be driven to zero by a fixed point iteration that works on the basis of Stefan Banach's Fixed Point Theorem [32] that was already applied in "Optimal Control" or "Model Predictive Control" e.g. in [33, 34]. The expected advantage could be that while the conditions $E(x_{min}) = 0$ in the minimum cannot be generally met, therefore Newton-Raphson algorithm can stop before reaching the absolute minimum, in it $\nabla E(x_{min}) = 0$ can be taken for granted, and no "stopping problems" have to be considered. Furthermore, by the introduction of format parameters depending on the "hight" of the location cylindrical samples of finite length can be considered in the numerically treatable range.

Acknowledgement
We acknowledge the financial support of this work by the Hungarian State and the European Union under the EFOP-3.6.1-16-2016-00010 project.

References

[1] J.V. Beck, B. Blackwell and C.R. St Clair Jr.: Inverse Heat Conduction, Wiley, New York, 1985

[2] A.N. Tikhonov and V.Y. Arsenin: Solution of Ill-Posed Problems, Winston, Washington DC., 1977

[3] O.M. Alifanov: Inverse Heat Transfer Problems, Springer, Berlin/Heidelberg, 1994

[4] M.N. Özisik and H.R.B. Orlande: Inverse Heat Transfer: Fundamentals and Applications, Taylor & Francis, New York, 2000.

[5] K.N. Prabhu and A.A. Ashish: Inverse modeling of heat transfer with application to solidification and quenching, Materials and Manufacturing Processes, 17(4):469-481, 2002

[6] I. Felde and T. Reti: Evaluation of hardening performance of cooling media by using inverse heat conduction methods and property prediction, STROJ VESTN-J MECH E, 56(2):77-83, 2010

[7] D. Landek, J. Župan and T. Filetin: A prediction of quenching parameters using inverse analysis, Materials Performance and Characterization, 3(2):229-241, 2014

[8] ISO 9950: Industrial Quenching Oils – Determination of Cooling Characteristics Nickel-Alloy Probe Test Method 1995(E), ISO, Switzerland, 1995

[9] J. Clark and R. Tye: Thermophysical properties reference data for some key engineering alloys, High Temperatures – High Pressures, 35-36:1:14, 2003-2004

[10] I. Felde: Estimation of thermal boundary conditions by gradient based and genetic algorithms, Materials Science Forum, 729:144-149, 2012

[11] S. Szénási, I. Felde and I. Kovács: Solving one-dimensional IHCP with particle swarm optimization using graphics accelerators, Proceedings of the 10th IEEE International Symposium on Applied Computational Intelligence and Informatics 2015, Timişoara, Romania, pp. 365-369, 2015

[12] I. Felde and S. Szénási: Estimation of temporospatial boundary conditions using a particle swarm optimisation technique, Int. J. Microstructure and Materials Properties, 11(3/4):288-300, 2016

[13] S. Szénási and I. Felde: Configuring Genetic Algorithm to Solve the Inverse Heat Conduction Problem, Acta Polytechnica Hungarica, 14(6):133-152, 2017

[14] S. Szénási and I. Felde: Using Multiple Graphics Accelerators to Solve the Two-dimensional Inverse Heat Conduction Problem, Computer Methods in Applied Mechanics and Engineering, 336:286-303, 2018

[15] L.A. Zadeh: Fuzzy Sets, Information and Control, 8:338-353, 1965

[16] A. Szeles, D.A. Drexler, J. Sápi, I. Harmati and L. Kovács: Model-based Angiogenic Inhibition of Tumor Growth using Adaptive Fuzzy Techniques, Periodica Polytechnica – Electrucal Engineering and Computer Science, 58(1):29-36, 2014

[17] J. Klespitz and M. Takács and I. Rudas and L. Kovács: Adaptive soft computing methods for control of hemodialysis machines, Proceedings of the iFuzzy2014 – 2014 International Conference on Fuzzy Theory and Its Applications, Kaohsiung, Taiwan, 2014.11.26–2014.11.28., pp. 109-112, 2014

[18] P. Szalay, L. Szilágyi, Z. Benyó and L. Kovács: Sensor Drift Compensation Using Fuzzy Interference System and Sparse-Grid Quadrature Filter in Blood Glucose Control, Lecture Notes in Comuter Science, 8835:445-453, 2014

[19] Umar Farooq, Jason Gu, Mohamed E. El-Hawary, Valentina E. Balas, Muhammad Usman Asad and Ghulam Abbas: Fuzzy Model-based Design of a Transparent Controller for a Time Delayed Bilateral Teleoperation System Through State Convergence, Acta Polytechnica Hungarica, 14(8):7-26, 2017

[20] J. Dombi: A general class of fuzzy operators, the De Morgan class of fuzzy operators and fuzziness measures induced by fuzzy operators, Fuzzy Sets and Systems, 8:149-163, 1982

[21] J. Bezanson, A. Edelman, S. Karpinski and V.B. Shah: Julia, `https://julialang.org`, Last time visited: 5 May 2019

[22] I. Felde: Liquid quenchant database: determination of heat transfer coefficient during quenching, Int. J. Microstructure and Materials Properties, 11(3/4):277-28, 2016

[23] J.Y. Shin, M.S. Kim and S.T. Ro: Correlation of Evaporative Heat Transfer Coefficients for Refrigerant Mixtures, Proceedings of the International Refrigeration and Air Conditioning Conference 1996 (Publisher: Purdue e-Pubs, Purdue University), Paper 316, pp. 151-156, 1996

[24] A. Cavallini, G. Censi, D. Del Col, L. Doretti, L. Rossetto and G.A. Longo: Heat Transfer Coefficients Of HFC Refrigerants During Condensation At High Temperature Inside An Enhanced Tube, Proceedings of the International Refrigeration and Air Conditioning Conference 2002 (Publisher: Purdue e-Pubs, Purdue University), Paper 563, 10 pages, 2002

[25] R. Mastrullo, A.W. Mauro, A. Rosato and G.P. Vanoli: Comparison of R744 and R134a heat transfer coefficients during flow boiling in a horizontal circular smooth tube, Proceedings of the International Conference on Renewable Energies and Power Quality (ICREPQ'09), 15th to 17th April, 2009, Valencia, Spain (Publisher: Purdue e-Pubs, Purdue University), 1(7):577-581, 2009

[26] J. Dombi and T. Jónás: Approximations to the normal probability distribution function using operators of continuous-valued logic, Acta Cybernetica, 23(3):829-852, 2018

[27] J. Dombi, T. Jónás and Z.E. Tóth: The epsilon probability distribution and its application in reliability theory, Acta Polytechnica Hungarica, 15(1):197-216, 2018

[28] J. Dombi, T. Jónás, Z.E. Tóth and G. Árva: The omega probability distribution and its applications in reliability theory, International Journal of Uncertainty, Fuzziness and Knowledge-Based Systems, 35(2):600-626, 2019

[29] J. Dombi and T. Jónás: Kappa regression: an alternative to logistic regression, International Journal of Uncertainty, Fuzziness and Knowledge-Based Systems, 28(2):237-267, 2020

[30] J.L. Lagrange, J.P.M. Binet and J.G. Garnier: Mécanique analytique (Analytical Mechanics), (Eds. J.P.M. Binet and J.G. Garnier), Ve Courcier, Paris, 1811

[31] Tjalling J. Ypma: Historical development of the Newton-Raphson method, SIAM Review, 37(4):531-551, 1995

[32] S. Banach: Sur les opérations dans les ensembles abstraits et leur application aux équations intégrales (About the Operations in the Abstract Sets and Their Application to Integral Equations), Fund. Math., 3:133-181, 1922

[33] H. Khan, J.K. Tar, I.J. Rudas and Gy. Eigner: Adaptive Model Predictive Control Based on Fixed Point Iteration, WSEAS Transactions on Systems and Control, 12:347-354, 2017

[34] H. Khan, J.K. Tar, I.J. Rudas and Gy. Eigner: Iterative Solution in Adaptive Model Predictive Control by Using Fixed-Point Transformation Method, International Journal of Mathematical Models and Methods in Applied Sciences, 12:7-15, 2018